Cellulose (2014) 21:1193–1204
DOI 10.1007/s10570-014-0184-8

ORIGINAL PAPER

Mixed solvents for cellulose derivatization under homogeneous conditions: kinetic, spectroscopic, and theoretical studies on the acetylation of the biopolymer in binary mixtures of an ionic liquid and molecular solvents

Haq Nawaz · Paulo A. R. Pires · Thaís A. Bioni · Elizabeth P. G. Arêas · Omar A. El Seoud

Received: 25 October 2013 / Accepted: 24 January 2014 / Published online: 12 February 2014

Abstract Rate constants for the acetylation of microcrystalline cellulose (MCC), by ethanoic anhydride in the presence of increasing concentrations of the ionic liquid (IL), 1-allyl-3-methylimidazolium chloride in dipolar aprotic solvents (DAS), *N*,*N*-dimethylacetamide (DMAC), and acetonitrile (MeCN), have been calculated from conductivity data. The third order rate constants showed a linear dependence on [IL]. We explain this result by assuming that the reacting cellulose is hydrogen-bonded to the IL. This is corroborated by kinetic data of the acetylation of cyclohexylmethanol, FTIR of the latter compound and of cellobiose in mixtures of IL/DAS, and conductivity of the binary solvent mixtures in absence, and presence of MCC. Cellulose acetylation is faster in IL/DMAC than in IL/MeCN; this difference is explained based on solvatochromic data (empirical polarity and basicity) and molecular dynamics simulations. Results of the latter indicate hydrogen-bond formation between the hydroxyl groups of the anhydroglucose unit of MCC, (Cl^-) of the IL, and the dipole of the DMAC. Under identical experimental conditions, acetylation in IL/DMAC is faster than that in LiCl/DMAC (2.7–8 times), due to differences in the enthalpies and entropies of activation.

Keywords Kinetics of Cellulose acetylation · Ionic liquids · Mixtures of ionic liquids with molecular solvents · 1-Allyl-3-methylimidazolium chloride · *N*,*N*-dimethylacetamide · Acetonitrile · Molecular dynamics simulation of cellulose dissolution

Introduction

An important consequence of the semi-crystalline nature of cellulose, with amorphous and crystalline domains, is that most dipolar aprotic solvents (DAS), cause cellulose swelling but not dissolution (Fidale et al. 2008). A notable exception is the strongly dipolar *N*-methylmorpholine-*N*-oxide-hydrate that dissolves the biopolymer; the latter is regenerated by precipitation in water to produce the so-called "Lyocell" fibers. (Perepelkin 2007). Addition of strong electrolytes, SE, e.g., LiCl and quaternary ammonium fluoride-hydrates to cellulose suspension in DAS, e.g., *N,N*-dimethylacetamide (DMAC) and dimethylsulfoxide (DMSO) causes cellulose dissolution. The reason is that the interactions between the electrolyte ions and the hydroxyl groups of the anhydroglucose glucose unit (AGU) disrupt the strong intra- and intermolecular hydrogen bonds present

Electronic supplementary material The online version of this article (doi:10.1007/s10570-014-0184-8) contains supplementary material, which is available to authorized users.

H. Nawaz · P. A. R. Pires · T. A. Bioni · E. P. G. Arêas · O. A. El Seoud (✉)
Institute of Chemistry, University of São Paulo, P. O. B. 26077, São Paulo, SP 05513-970, Brazil
e-mail: elseoud@usp.br

in cellulose, leading to its dissolution. Of these, the interactions (anion···H–O–AGU) are most important, although the nature of the cation plays a role (El Seoud et al. 2013). Ionic liquids (ILs) are composed only of ions and, by operational definition, have melting points <100 °C. There are several reasons for the explosive interest in the use of ILs as solvents for cellulose dissolution, regeneration, and derivatization. Being ionic in nature, there is no need for an additional electrolyte, e.g., LiCl, for cellulose dissolution; no pretreatment, e.g., thermal, is required for biopolymer activation. The most important advantage, however, is their structural versatility because an unlimited number of molecular structures can be generated by combinations of different cations and anions (El Seoud et al. 2007; Gericke et al. 2012).

The use of ILs is associated with some limitations. Based on the current catalog of a reagent supplier, the cost of 1 mol of 1-allyl-3-methylimidazolium chloride, AlMeImCl, the IL of interest in the present work, is ca. ten times greater than 1 mol of a LiCl solution in DMAC. Relative to the SE/DAS employed with cellulose, the viscosities of many ILs are high. For example, at 80 °C the zero-shear viscosity of the structurally related IL 1-allyl-3(1-butyl)imidazolium chloride, AlBuImCl, is 36.4 times that of 8 % LiCl/DMAC. Dissolution of 5 wt% of MCC (the same sample employed in the present work) in AlBuImCl increases the viscosity, relative to that of pure IL, by factors between 6.3 and 11.6, depending on the temperature, T. At 25 °C, the viscosity of 5 wt% of MCC, in AlBuImCl is ca. 6.7 times that of 5 wt% MCC/LiCl-DMAC (Possidonio et al. 2010). These differences in viscosity are relevant to cellulose derivatization in *any* solvent because lower viscosity favors the reaction due to the concomitant increase in reagent diffusion rate, as given by the Einstein-Stokes equation (Berry et al. 2000). In view of the documented favorable effects of lower viscosity on the accessibility of amino acid residues of some enzymes [(a) Somogyi et al. 1988; (b) Punyiczki and Rosenberg 1992] and on the rate constants of enzymatic reactions (Sitnitsky 2008), it is clear that lower medium viscosity should lead to enhanced cellulose accessibility/reactivity. Finally, some reagents for synthesis of cellulose carboxylic esters (e.g., long-chain acid anhydrides) are immiscible with certain ILs.

In principle, many of these limitations can be attenuated/eliminated by using mixtures of IL and DAS that are efficient in cellulose swelling, e.g., DMSO and DMAC (Gericke et al. 2011). This use is still incipient, calling for extensive studies in order to determine the binary mixture compositions that are best for a given class of reactions, e.g., esterification. An important impetus for these studies is the fact that many of the properties of binary solvent mixtures that are relevant to cellulose dissolution/derivatization, e.g., empirical polarity, acidity, basicity, and viscosity do not vary linearly as a function of mixture composition (Sato et al. 2010; Hauru et al. 2012; Le et al. 2012). Therefore, more research is necessary to understand the properties of the IL-molecular solvent binary mixtures and how their interactions with cellulose affect accessibility of the latter, hence its reactivity. There is also need to assess the efficiencies of these solvent mixtures with those of the "classical" and extensively employed SE/DAS.

We have carried out the present study with this background in mind. Using conductivity, we have studied the kinetics of acetylation of MCC, in mixtures of AlMeImCl (hereafter designated as IL) and DAS, namely DMAC and acetonitrile, MeCN. Surprisingly, values of the third order rate constants were found to be dependent on the concentration of the IL, a fact attributed to its efficient hydrogen-bonding with the hydroxyl groups of the AGU. The order of reactivity was found to be IL/DMAC>LiCl/DMAC>IL/MeCN, because of differences in the corresponding activation parameters.

Experimental

Solvents and reagents

All solvents and reagents were purchased from Alfa Aeser or Merck and were purified as recommended elsewhere (Armagero and Chai 2003). The purity of the molecular solvents was established from their density (DMA 4500 M resonating-tube densimeter; Anton Paar) (Lide 2004) and empirical polarity, $E_T(33)$ in kcal mol^{-1}, as determined by the solvatochromic indicator 2,6-dichloro-4-(2,4,6-triphenyl-1-pyridinio)phenolate, WB (Tada et al. 2000). MCC (Avicel PH 101) was obtained from FMC, Philadelphia (degree of polymerization by viscosity, DPv = 150) (ASTM 2001); index of crystallinity, Ic, by X-ray diffraction = 0.82 (Buschle-Diller and Zeronian 1992). Ethanoic anhydride, Ac_2O, was

distilled from P_4O_{10} under reduced pressure; allyl chloride was purified by washing with dilute HCl, and then with aqueous base (Na_2CO_3), water, followed by drying on anhydrous $MgSO_4$ and distillation. *N*-Methylimidazole; cyclohexylmethanol, CHM, *trans*-1,2-cyclohexanediol, CHD, were distilled from CaH_2.

Microwave-assisted synthesis of AlMeImCl

This synthesis was carried out as given elsewhere from the reaction of *N*-methylimidazole (40 mL; 0.501 mol) and allyl chloride (43 mL; 0.527 mol) under microwave irradiation.(Sato et al. 2010) The product gave the expected ^{1}H NMR spectrum (Varian Innova-300 NMR spectrometer) and its solution in water showed the absence of acid or base impurity (expanded-scale pH paper). Pure AlMeImCl was stored in tightly-stoppered bottles. The density of the IL (1.14108 g cm^{-3}) was determined by the above-mentioned density meter.

Dissolution of cellulose in mixtures of IL and DAS

MCC (0.7 g, 43.2 mmol) was weighed into a three-necked round-bottom flask fitted with magnetic stirrer and 100 mL graduated addition funnel (no equilibration side arm) containing the appropriate volume of pure IL (36.7 mL (41.88 g)–73.6 mL (83.98 g), and 51.53 mL (58.8 g)–73.6 mL) for mixtures of IL with DMAC and MeCN, respectively. The flask was connected to a vacuum pump (2 mmHg) and heated to 110 °C in ca. 30 min, and then kept under these conditions for additional 45 min. While maintaining the reduced pressure, the IL was slowly introduced, with continuous stirring. The mixture (MCC plus IL) was kept under these conditions for additional 20 min, and then the pressure was brought to atmospheric with dry, oxygen-free nitrogen. The temperature was decreased to 80 °C in 1 h, and the mixture was stirred at this temperature for additional 3 h. The DAS, was slowly added with continuous stirring; 50 mL (lowest IL content) to 10 mL (highest IL content) of DMAC, or 30–10 mL of MeCN. The resulting clear solution was transferred into 100 mL volumetric flask and the volume was completed up to the mark with DAS (ca. 10 mL) that has been employed to wash the addition funnel and the round-bottom flask. All solutions of MCC/IL-DAS were clear and isotropic, as indicated by examination between two Polaroid plates against light.

Kinetics of acetylation of the model compounds CHM and CHD and of MCC

The progress of the acetylation reaction was monitored by following the increase in solution conductivity (λ) as a function of time (t), at a constant (T). We have employed a PC-controlled Fisher Accumet AR-50 ion meter equipped with Metrohm 6.0910.120 conductivity electrode and a glass-covered PT-100 temperature sensor. These are inserted in a double-walled conductivity cell through which water is circulated from a thermostat, and attached to a computer via RS-232 serial port, as shown elsewhere (Nawaz et al. 2012, 2013).

We have carried out the kinetic experiments as follows: 10 mL of the solution of the compound to be studied (MCC, CHM, or CHD) in the appropriate solvent (IL-DAS) were introduced into the conductivity cell; the latter was quickly closed, and heated to the desired temperature (30–60 °C). After thermal equilibration, 4 mL of a solution of Ac_2O/DAS was added. The *final* concentrations of the reactants in the conductivity cell (14 mL, assuming no volume change on mixing) were, in mol L^{-1}: CHM = 0.0308; CHD = 0.0616; MCC = 0.0924; acetic anhydride = 1.057. The *final* IL concentrations in the conductivity cell were, in mol L^{-1}: 1.887, 2.269, 2.647, 3.025, 3.404, 3.782 (IL-DMAC); and 2.647, 3.025, 3.404, 3.782 (IL-MeCN). After adding the anhydride, the increase in (λ) was recorded as a function of (t). We have employed a home-developed non-linear regression analysis program for calculating the values of the observed rate constants (k_{obs}). This calculation is based on minimizing the sum of the squares of the residuals (=differences between experimental and calculated λ) using Marquardt–Levenberg algorithm (Press et al. 2007). The agreement between calculated and experimental "infinity" conductivity (λ_∞) was routinely checked. Values of (k_{obs}) were calculated from the slopes of plots of ln ($\lambda_\infty - \lambda_t$) versus (t), these were strictly linear, as shown in Figure *ESM*-1 (Fig. 1 of Electronic Supplementary Material; file Online Resource 1). The relative standard deviation in k_{obs}, i.e., ((standard deviation/k_{obs}) × 100), was ≤0.5, that between k_{obs} of triplicate runs was <3 %. Values of the third-order rate constants (k_3) were obtained by dividing the corresponding k_{obs} by {[Ac_2O] × [IL]}. The activation parameters were calculated from the dependence of k_3 on T, by using

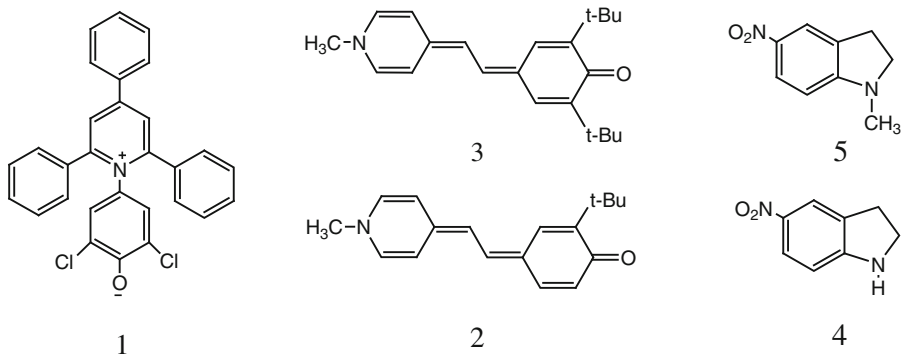

Fig. 1 Molecular structures of the probes employed for the determination of the solvatochromic properties of the solvents. These include: 2,6-dichloro-4-(2,4,6-triphenyl-1-pyridinio)phenolate, WB (**1**); *o-tert*-butylstilbazolium betaine (**2**), and *o*,*o*′-di-*tert*-butylstilbazolium betanie (**3**); 5-nitroindoline (**4**), and 1-methyl-5-nitroindoline (**5**). The solvent descriptors determined by these probes are, respectively: microscopic polarity; solvent acidity, and solvent basicity

standard equations (Anslyn and Dougherty 2006). Details of the experimental conditions employed for each compound are listed in Tables *ESM-1 and ESM-2*.

Synthesis of cellulose acetate under conditions of the kinetic experiment

We repeated the kinetic experiments on a threefold scale in a three-necked round-bottom flask. After MCC dissolution, vide supra, cellulose was reacted with ethanoic anhydride ($Ac_2O/AGU = 4.5$), under the following conditions: 1.887 mol L^{-1} IL/DMAC, 30 min at 40 °C; 2.647 mol L^{-1} IL/MeCN, 2 h at 40 °C. The resulting solutions were added to ethanol; the solid precipitated was repeatedly suspended in the same solvent (3 × 200 mL; 60 °C), then filtered, washed with water, and dried at 60 °C for 24 h, under reduced pressure, over P_4O_{10}. The products gave IR spectra (Vector 22 FTIR spectrophotometer; KBr pellet) similar to authentic cellulose acetate. The degrees of substitution, DS, of the esters were determined by titration (ASTM 2002); they were found to be 2.39 and 2.47, for the reaction IL-DMAC and IL-MeCN, respectively.

Effect of AlMeImCl on the IR stretching frequency, $\nu_{(OH)}$, of CHM and cellobiose

We have employed the following conditions to determine the effect of the IL on (ν_{OH}), the stretching frequency of the hydroxyl group of CHM, or cellobiose: CaF_2 cell, 0.025 mm path width; 32 spectra accumulated at 0.5 cm^{-1} resolution. The *final* concentrations, in the IR cell were in mol L^{-1}: CHM = 0.3 and IL = 0.086, in DMAC or MeCN. We carried out a similar experiment on a solution containing 0.086 and 0.172 mol L^{-1} cellobiose, and IL, respectively in DMSO. We have employed the latter instead of DMAC because of cellobiose solubility problem.

Determination of the properties of the reaction media by solvatochromic dyes

The molecular structures of the solvatochromic dyes employed (hereafter designated as probes) are shown in Fig. 1. The probes and solvent descriptors that we have calculated from their UV–vis spectra (Shimadzu UV 2550 spectrophotometer, at 40 °C) are: WB (1), empirical polarity, $E_T(33)$ in kcal mol^{-1}; *o-tert*-butylstilbazolium betaine (2) and *o*,*o*′-di-*tert*-butylstilbazolium betanie (3) solvent acidity (SA); 5-nitroindoline (4) and 1-methyl-5-nitroindoline (5), solvent basicity (SB). Aliquots of each probe solution in methanol (2 mL) were pipetted into 10 mL glass vials. The alcohol was evaporated under reduced pressure in the presence of P_4O_{10}. Aliquots of the solution to be tested (1 mL) were pipetted into the vials containing the solid, dry probe. The latter was dissolved (final probe concentration = $0.75 - 1.5 \times 10^{-3}$ mol L^{-1}), the solution transferred into 1 cm path cell, and its

absorbance was recorded. We have calculated the values of $E_T(33)$, SA, and SB from the values of λ_{max}, calculated from the first derivative of the spectra, as outlined elsewhere (Tada et al. 2000; Catalán 2009).

Molecular dynamics, MD, simulations

These were carried out by using Gromacs 4.5.5 software package (Van der Spoel et al. 2005). Two systems were simulated, each containing 1 molecule of AGU oligomer, composed of 12 AGUs (dodecaose; hereafter designated as "oligomer"), 301 molecules of the IL, and 1,143 molecules of the DAS. The simulation was performed at 300 K, for 75 ns by using GAFF (General Amber Force Field) (Wang et al. 2004), isothermal-isobaric (NPT) ensemble periodic boundaries, and the smooth particle-mesh Ewald (PME) algorithm for long-range electrostatic interactions (Jorgensen et al. 1996). The IL has its geometry optimized (gas phase) by using DFT calculation, by employing "good-opt" parameter using the Orca 2.9 program (Neese et al. 2011). The oligomer chain was drawn using Cellulose-Builder script (Gomes and Skaf 2012). Partial charges on the atoms were calculated using the RESP (Restrained ElectroStatic Potential fit) approach (Bayly et al. 1993) as calculated by the RED (RESP ESP charge Derive) on-line server (Vanquelef et al. 2011). The topologies files for GAFF were generated by using the Acpype (Silva and Vranken 2012) and Antechamber 12 programs (Wang et al. 2006). GAFF-optimized geometries and topologies of DMAC and MeCN were taken from literature (Wang et al. 2004; Caleman et al. 2012) and the simulation boxes were generated using Packmol program (Martínez et al. 2009). We have checked the equilibration of the ensemble by monitoring the potential energy as a function of simulation time plot; the latter reached equilibrium, i.e., remained essentially constant, after ca. 15 ns until the end of simulation (75 ns). Analysis of the results of MD simulations was done through the use of radial distribution functions (RDF) or by H-bond calculations made by using visual molecular dynamics (VMD) software (Humphrey et al. 1996).

Results and discussion

The objective of the present study is to assess the efficiency of IL-DAS mixtures as solvents for cellulose dissolution and derivatization, as compared with the "classic" system LiCl/DMAC. We have calculated (for the first time) the rate constants and activation parameters for cellulose acetylation as a function of [IL]; T, and the DAS employed, DMAC or MeCN.

As given in Experimental, we have carried out the kinetic runs under pseudo-first-order conditions, with the following molar concentration ratios: (Ac_2O/cellulose) = 11.44; (IL/cellulose) = 20.41–40.93 (reaction in IL-DMAC) and 28.6–40.9 (reaction in IL-MeCN). As shown in Figure *ESM*-1, excellent linear plots were observed for $\ln(\lambda_\infty - \lambda_t)$ versus (t) in all cases, showing that the reaction is first order in cellulose. The value of (k_3) was then calculated as indicated in Experimental. As discussed elsewhere (Nawaz et al. 2012, 2013), (k_3) refers to the reaction of one primary hydroxyl-, Prim(OH), and two secondary hydroxyl groups, Sec(OH) of the AGU. In order to separate (k_3) into its individual components, we have employed CHM as a model for C6–OH, and CHD as a model for C2–OH plus C3–OH of the AGU. For simplicity, we consider that C2–OH and C3–OH have the same reactivity, as suggested elsewhere (Malm et al. 1953; Kwatra et al. 1992; Tosh et al. 2000), i.e.

$$k_3 = k_{3,\mathrm{Prim(OH)}} + 2k_{3,\mathrm{Sec(OH)}} \quad (1)$$

Equation (1) can be split into contributions from Prim(OH) and Sec(OH) if the ratio (χ) between the rate constants of both hydroxyl types is known. We have employed the reactivities of CHM and CHD toward acetylation to mimic those of the corresponding hydroxyl groups of the AGU. Under the same experimental conditions (1.887 mol L^{-1} IL in DMAC, T = 60 °C); we have obtained (k_{obs}) of 7.06×10^{-4} s^{-1} and 4.22×10^{-4} s^{-1} for the acetylation of CHM and CHD, respectively, giving $\chi = k_{obs,Prim(OH)}/k_{obs,Sec(OH)} = 1.67$. This ratio is within the range 1.30–1.80 that we have calculated for uncatalyzed- and imidazole-catalyzed acetylation of the same compounds in LiCl-DMAC. As we have argued previously, this ratio is smaller than that observed for the derivatization of cellulose under *heterogeneous* reaction conditions (4 ± 1) (Malm et al. 1953; Kwatra et al. 1992; Jain et al. 1985), most probably due to difference in accessibility of hydroxyl groups of the model compounds (totally accessible) and cellulose (primary hydroxyls are more accessible than secondary ones). Therefore, depending on the

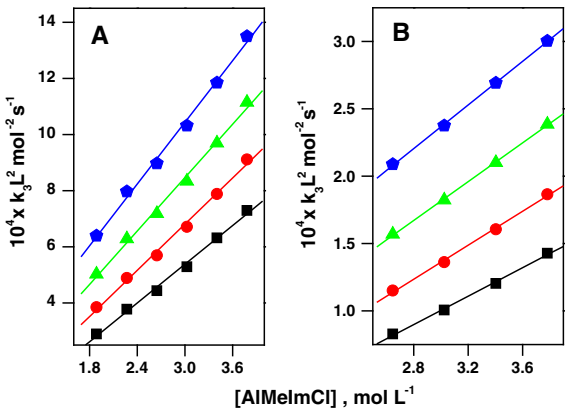

Fig. 2 Dependence of overall k_3 on [IL] in the systems IL-DMAC (part **A**) and IL-MeCN (part **B**). *Square*, *Circle*, *Triangle* and *Pentagon* are for k_3 at 30, 40, 50 and 60 °C, respectively

conditions of the reaction the limits of (χ) lie between 1.3 and 5. We have divided (k_3) using these limiting ratios, as well as their arithmetic mean, 3.15, see Tables *ESM*-4 and *ESM*-5. These show, as expected, that the order of reactivity is: primary (OH) > secondary (OH). Additionally, the use of different (χ) to split (k_3) does not affect the activation enthalpy; the variation in the activation entropy term and the free energy was ≤1.46 %.

Tables *ESM*-1 and *ESM*-2, show the values of k_{obs} (in s^{-1}) and k_3 (in L^2 mol^{-2} s^{-1}) for the acetylation of MCC in the presence of different concentrations of IL, at different temperatures in mixtures of the IL with both DAS; plots of the dependence of k_3 on [IL] are depicted in Fig. 2.

Regarding these results, the following is relevant:

1. *Proof that the observed increase in conductivity is due to cellulose acetylation*

Although conductivity (λ) is a convenient technique to determine rate constants, independent evidence is required to show that the increases in (λ) as a function of (t) is due to cellulose acetylation. We have confirmed this by carrying out the reaction on a larger scale, *under the kinetic conditions*, followed by product isolation and purification. Cellulose acetate was obtained, see Experimental;

2. *Rationale for the unexpected dependence of (k_3) on the concentration of IL*

Surprisingly, the values of (k_3) were found to increase linearly as a function of [IL] as shown in Fig. 2. This dependence is not restricted to MCC, it has also been observed for CHM, as shown in Figure *ESM-2*. We advance several reasons to explain this result:

- The IL is present as aggregate in the binary solvent mixture.

The results of several experimental techniques, including FTIR, (Jiang et al. 2011) conductivity (Bester-Rogac et al. 2011) and NMR spectroscopy (Hesse-Ertelt et al. 2010; Ananikov 2011) have indicated the association of ILs in several DAS. Thus, higher kinetic order in [IL] may be observed;

- The biopolymer is solvated by the IL, via hydrogen bonding and dipolar interactions.

The above-mentioned techniques, as well as cellulose solubility measurements and theoretical calculations have clearly indicated the strong interactions of cellulose-IL/DAS (El Seoud et al. 2007; Sashina et al. 2008; Pinkert et al. 2009; Arvela et al. 2010; Gericke et al. 2012). It is more likely, therefore, that cellulose is reacting as (cellulose-IL) hydrogen-bonded species, akin to the alcohol-IL complexes (Crosthwaite et al. 2005; Makowska et al. 2010) and water-IL complexes (Sato et al. 2012); this leads to the dependence of (k_3) on [IL].

In order to corroborate the formation of (IL···AGU) hydrogen bonding, we have examined the systems by FTIR and conductivity. In DMAC, the stretching frequency of the hydroxyl group, ν_{OH}, of 0.3 mol L^{-1} solution of CHM decreased from 3,433 to 3,416 cm^{-1} in the presence of 0.086 mol L^{-1} IL; the corresponding figures for MeCN are 3,538 and 3,535 cm^{-1}, respectively. Likewise, the co-solubilization of 0.172 mol L^{-1} of the IL decreased ν_{OH} of 0.086 mol L^{-1} cellobiose from 3,332 to 3,313 cm^{-1} (experiment carried out in DMSO, because of cellobiose solubility problem in DMAC and MeCN).

The results of the conductivity measurements are shown in Fig. 3.

In most cases, the dependence of (λ) on [IL] is linear; for the same IL concentration, the value of $\lambda_{(IL/DMAC)} > \lambda_{(MCC\text{-}IL/DMAC)}$, probably because the mobility of the free chloride ion of the IL is larger than that of the Cl^-···H–O-AGU.

We have considered another factor, the effect of adding IL on the microscopic solvent properties of the medium. This can be accessed from the

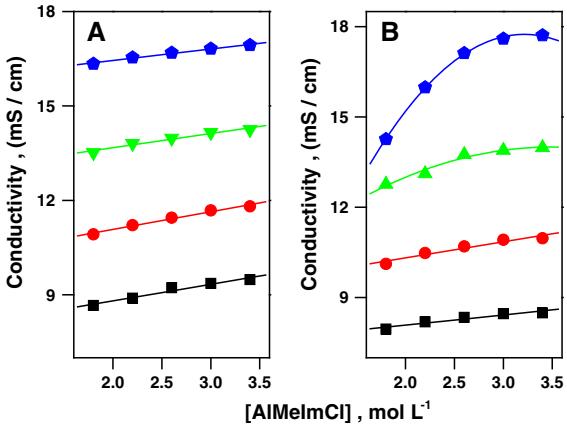

Fig. 3 Dependence of solution conductivity on [IL] in the systems IL-DMAC (part A) and MCC-IL-DMAC (part B) in the presence of a fixed concentration of MCC, 0.0924 mol L^{-1}. *Square*, *Circle*, *Triangle* and *Pentagon* shows conductivity at 30, 40, 50 and 60 °C respectively

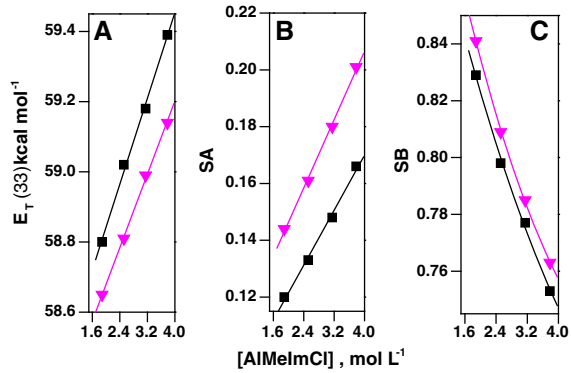

Fig. 4 Dependence of solvent properties on [IL]: polarity, $E_T(33)$, (part **A**), acidity (part **B**) and basicity (part **C**); in IL-DMAC (*square*) and in MCC-IL-DMAC (*triangle*) mixtures. All parameters are calculated from data at 40 °C

solvatochromic parameters shown in Fig. 4 (and Table *ESM-6*) for the systems IL/DMAC and MCC-IL/DMAC.

As can be seen from Table *ESM-6*, the initial addition of IL causes a huge increase in the empirical polarity of DMAC, followed by small, but persistent increase as a function of increasing [IL]. This behavior may be due to preferential solvation of the polarity probe by IL, or (IL···DMAC), as explained elsewhere (El Seoud et al. 2007, 2009). Solvent acidity of pure DMAC is close to zero because this DAS carries no acidic hydrogen (Catalán 2009). Addition of the IL, however, leads to initial large increase in SA, because of the presence of the relatively acidic C2–H in the imidazolium heterocycle. Again, the subsequent increase in (SA) is much smaller as a function of [IL]. Introduction of the IL, with its acidic C2–H leads to a decrease in medium basicity.

The effect of co-dissolution of MCC on the solvatochromic parameters is small, indicating that solvation of the probes employed is dominated by its hydrogen-bonding and dipolar interactions with the IL or IL-DAS. Therefore, the initial large variations in the solvatochromic parameters on dissolving the IL clearly show that the microscopic properties of the medium, that are relevant to cellulose dissolution and accessibility, have been perturbed. Analysis of increasing [IL] on solution viscosity, hence on k_3, is outside the scope of the present work. It sufficient to note, however, that the viscosities of IL-DAS mixtures increase as a function of increasing [IL] (Ciocirlan et al. 2011). As this is expected to decreases the reactant diffusion coefficients, vide supra, then rate enhancement due to cellulose-IL bonding must out weight the (adverse) effect of the accompanied increase in solution viscosity.

In summary, the dependence of (k_3) on [IL] may be due to two factors: (a) the formation of (MCC···IL) or (CHM···IL) hydrogen bonds, and (b) the change in the microscopic properties of binary solvent mixture, because of the large volume fractions of IL.

3. *Effects of the nature of the DAS*

As Fig. 2 and Tables *ESM-3 to ESM-5* show, values of overall (k_3), and consequently of $k_{3,Prim(OH)}$ and $k_{3,Sec(OH)}$ are larger for IL-DMAC than for IL-MeCN. At each [IL], the differences in (k_3) decrease slowly as a function of increasing T (see values within parenthesis of Table *ESM-3*). A rationale for effect of the nature of the DAS can be deduced by examining the differences between the activation parameters. These are listed in the part of MCC-IL/MeCN of Table *ESM-3*, as the difference (ΔΔ activation parameter = activation parameter for IL/MeCN—activation parameter for IL-DMAC). Consider first $\Delta\Delta H^{\neq}$; all differences are positive, i.e., the reaction in IL-DMAC has a lower enthalpy of activation, ranging from 0.86 to 1.49 kcal mol^{-1}. As usual for associative reactions (cellulose-IL/DAS-acid anhydride) there is a decrease in the degrees of freedom in going from reagents to the transition state, i.e., the $T\Delta S^{\neq}$ term is negative (Bruice 2006). Although all $\Delta T\Delta S^{\neq}$ are positive (the entropy

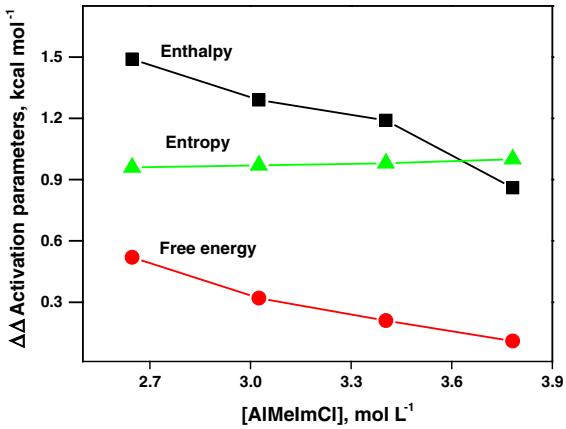

Fig. 5 Dependence of the difference in activation parameters on [IL]. *Square* ($\Delta H^{\neq}$ IL/MeCN − $\Delta H^{\neq}$ IL/DMAC), *triangle* ($\Delta G^{\neq}$ IL/MeCN − $\Delta G^{\neq}$ IL/DMAC) and *circle* ($T\Delta S^{\neq}$ IL/MeCN − $T\Delta S^{\neq}$ IL/DMAC). The activation parameters were calculated at 60 °C

term for the reaction in IL-MeCN is more favorable) their *absolute* values are smaller than those of $\Delta\Delta H^{\neq}$. That is, the reaction in IL-DMAC is faster due to gain in activation enthalpy, not compensated by loss in the $T\Delta S^{\neq}$ term. As an example, consider the reaction in the presence of 2.647 mol/L IL. It is faster in IL-DMAC because $\Delta G^{\neq}$ is lower by 0.96 kcal mol^{-1}, due to gain in $\Delta H^{\neq}$ (1.49 kcal mol^{-1}) and loss in $T\Delta S^{\neq}$ (0.52 kcal mol^{-1}). Figure 5 summarizes the *differences* between the activation parameters, calculated at 60 °C as a function of [IL].

The effect of DAS on reactivity can be explained, based on the following:

- *Differences in the microscopic properties of the DAS proper*

As given in Table *ESM-6*, the solvatochromic properties of both DAS are different. Whereas MeCN is more polar than DMAC ($E_T(33)$), the latter solvent is much more basic (SB), i.e., is more efficient in hydrogen bonding to the hydroxyl groups of the AGU; this leads to more accessible biopolymer. The importance of medium basicity to cellulose dissolution/regeneration and, presumably, accessibility is well documented (Hauru et al. 2012).

- *Stronger interactions of the biopolymer with IL/DMAC*

We have carried out MD simulations in order to compare the interactions of cellulose with IL and

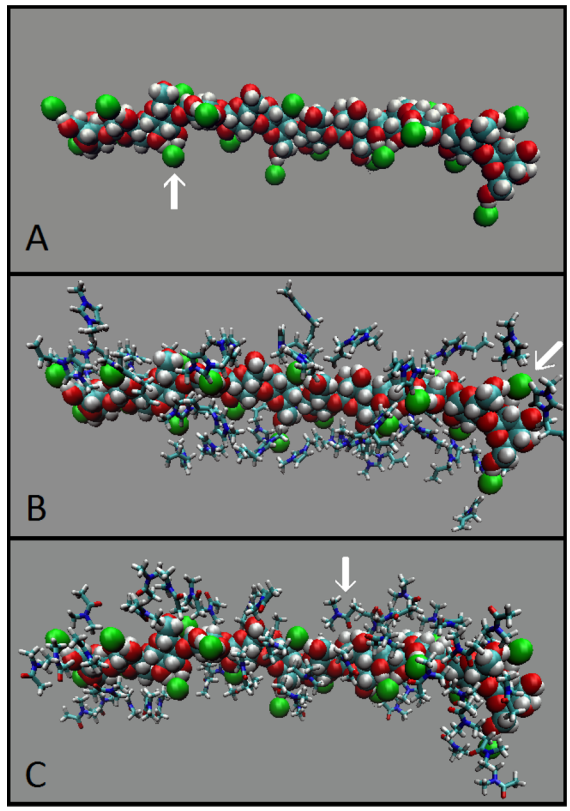

Fig. 6 Snapshot of an MD simulation frame showing the oligomer and its first solvation shell (0.47 nm). Part (**A**) shows the oligomer plus (Cl^-). The *arrow* shows that this anion forms *simultaneous* hydrogen-bonds to two OH groups of the AGU. Part (**B**) shows the oligomer plus (Cl^-) and Imz^+. The *arrow* shows two Imz^+ hydrogen-bonded to a single (Cl^-) via their C2–H. Part (**C**) shows the oligomer plus (Cl^-) and DMAC. The *arrow* indicates the hydrogen bonding between C=O of DMAC and the OH of the AGU

DMAC or MeCN. To our knowledge, this is the first time that such simulations have been employed to probe the interactions of cellulose with these binary solvent mixtures. As a model for cellulose, we have employed glucose dodecamer (hereafter designated as "oligomer"); the systems studied included one oligomer, 301 molecules of IL and 1,143 molecules of the DAS. Figure 6 and Table 1 summarizes the main results of these calculations.

Regarding these data, the following is relevant

- Calculation of the radial distribution function, RDF, of all atoms present around the oligomer surface has indicated that the extension of its solvation layer can be taken as equal to 0.47 nm; this value has been employed throughout. In what

Table 1 Results of molecular dynamics simulations of the system oligomer/IL-DAS

Entry	Pairs of interacting species	DMAC/IL		MeCN/IL	
		Solvation shell extension (nm)[a]	Number of interacting species[a]	Solvation shell extension, (nm)[a]	Number of interacting species[a]
1.	DAS COM and oligomer surface	From 0.224 to 0.564, maximum at 0.444	**48.48** DMAC/oligomer 3.79 DMAC/AGU	From 0.216 to 0.476, maximum at 0.398	**35.17** MeCN/oligomer 2.93 CH_3CN/AGU
2.	Cl^- and oligomer surface	From 0.156 to 0.238, maximum at 0.182	**18.64** Cl^-/oligomer 1.55 Cl^-/AGU	From 0.156 to 0.236, maximum at 0.184	**20.87** Cl^-/oligomer 1.74 Cl^-/AGU
3.	IMZ^+ COM and oligomer surface	From 0.184 to 0.748, maximum at 0.396	**45.35** IMZ^+/oligomer 3.78 IMZ^+/AGU	From 0.204 to 0.734, maximum at 0.380	**49.89** IMZ^+/oligomer 4.16 IMZ^+/AGU

COM center of mass

[a] The numbers and distances of the species are average values, calculated for the simulation time interval 15–70 ns

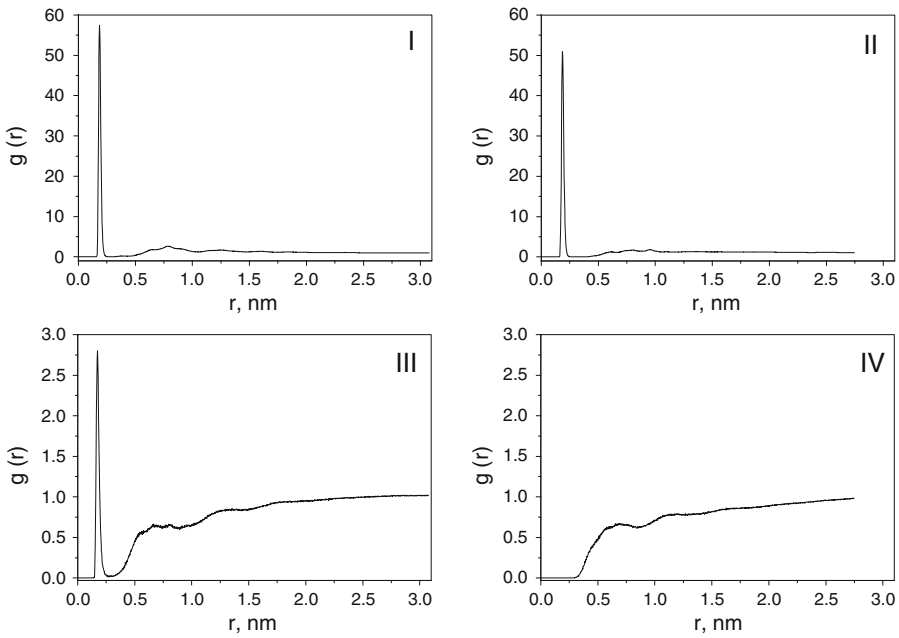

Fig. 7 Parts (**I**) and (**II**) show the radial distribution function, RDF (g(r)) of (Cl^-) around the HO-AGU of the oligomer, in DMAC, and MeCN, respectively. Parts (**III**) and (**IV**) show the RDF of the DAS around the HO–AGU of the oligomer, in DMAC, and MeCN, respectively

follows, *all values given are average*, taken within the solvation layer;

- We dwell on the interactions between HO–AGU and the binary mixture components, because these are the interactions relevant to cellulose accessibility, hence reactivity;
- The arrows inserted in Fig. 6 clearly indicate the formation of hydrogen-bonds in the system. Part (A) shows this bonding between (Cl^-) and two hydroxyl groups of the AGU. This *simultaneous* bonding explains the efficiency of ILs as solvents for cellulose and other biopolymers. It agrees with parts (I) and (II) of Fig. 7 below, where the sharp peak of the RDF curve clearly indicates strong (Cl^-···HO-AGU) interactions in both solvents. The arrow in part (B) of Fig. 6 shows the importance of C2-H to bonding of the ions of the IL proper. This agrees with the interpretation of the results of MD simulations by other authors (Dong et al. 2006; Hanbin et al. 2010). Part (C) of Fig. 6

Table 2 Rate constants (overall k_3) and activation parameters for the acetylation of MCC in LiCl-DMAC; IL-DMAC, and IL-MeCN

Reaction medium, k_3 (L^2 mol^{-2} s^{-1}/T)	40 °C	50 °C	60 °C	$\Delta H^{\neq a}$ (kcal mol^{-1})	$T\Delta S^{\neq a}$ (kcal mol^{-1})	$\Delta G^{\neq a}$ (kcal mol^{-1})
LiCl/DMAC	0.675	0.928	1.250	5.72	−19.80	25.52
IL/DMAC	1.346	2.150	3.139	5.41	−19.39	24.80
IL/MeCN	0.104	0.378	0.751	7.26	−18.55	25.82

At a constant electrolyte concentration of 1.007 mol L^{-1}

All rate constants should be multiplied by 10^{-4}

The values in this table are extrapolated from dependence of the activation parameter on [IL] using data from Table *ESM-3*

[a] Activation parameters were calculated for the reaction at 60 °C. The uncertainties in the activation parameters are ±0.05 kcal mol^{-1} ($\Delta H^{\neq}$, and $\Delta G^{\neq}$) and 0.2 cal K^{-1} mol^{-1} ($T\Delta S^{\neq}$)

shows the participation of DMAC in further hydrogen bonding to the hydroxyl of AGU.

- The importance of SB of the DAS is apparent from two pieces of evidence: Entry 1 of Table 1 shows that the number of DMAC molecules at the surface of the oligomer exceeds that of MeCN by 37.8 %, although volume of the former is 90.6 % larger than that of MeCN (0.1308 and 0.0686 nm^3 molecule^{-1}, for DMAC and MeCN, respectively). Additionally, in Fig. 7 the sharp RDF peak in (III) indicates the presence of strong interactions between the C=O of DMAC and HO–AGU. On the other hand, this peak is absent in the RDF curve of (IV), indicating much weaker interactions between HO–AGU and MeCN;
- Entries 2 and 3 of Table 1 show that the number of ions of the IL at the surface of the oligomer are slightly less in case of DMAC than MeCN, being 89.3 and 90.9 % for Cl^- and Imz^+, respectively. This reflects the finite volume of the oligomer solvation shell, and the fact that it contains a larger number of DMAC molecules. In other words, this should not be taken to indicate weaker interactions between the IL and the oligomer in case of DMAC.

In summary, our MD simulations show that the oligomer interactions with both solvent components are stronger for LI/DMAC than LI/MeCN. Thus biopolymer solvation in the former solvent system is more extensive, being associated with better accessibility, hence higher reactivity.

4. *Comparison of the IL/DAS system with LiCl/DMAC as solvents for cellulose derivatization*

Table 2 shows the rate constants (overall k_3) and the corresponding activation parameters for the acetylation of MCC by acetic anhydride; all data were calculated at the same electrolyte concentration of 1.007 mol L^{-1}. Where required, the values of (k_3) were calculated by extrapolation from the present work, and that on acetylation in LiCl/DMAC (Nawaz et al. 2012). At 40 °C, the ratio k_3 IL-DMAC/k_3 LiCl-DMAC is ca. 8, decreasing to 2.7 at 60 °C. This may be attributed to the effect of increasing temperature on the dissociation of the tightly-bound ion pair of LiCl, relative the loosely-bound ions of the IL. The rate enhancement by IL/DMAC, relative to LiCl/DMAC is due to slightly favorable $\Delta H^{\neq}$ (0.54 kcal mol^{-1}) and $T\Delta S^{\neq}$ (ca. 0.1 kcal mol^{-1}). Note, however, that the use of IL-DAS as solvent for the derivatization of cellulose is less energy demanding because the biopolymer dissolves faster than in LiCl/DMAC (typically overnight stirring and heating is required for the latter); biopolymer activation, e.g., by drying under reduced pressure, is not required for IL-DAS because it does not affect DS of the esters (Fidale et al. 2009).

Conclusions

The reactant in the acetylation reaction is most probably cellulose hydrogen-bonded to the IL. This conclusion is supported by the dependence of (k_3) on [IL]; FTIR spectroscopy; conductivity measurements, and MD simulations. The latter have indicated stronger interactions of cellulose with both components of the IL/DMAC medium, as compared with IL/MeCN. The effect of the nature of DAS can be traced to its basicity. Given its low cost and efficiency, LiCl/DMAC is a good choice for cellulose dissolution and

subsequent derivatization. The IL/DAS system is less energy demanding, no cellulose pre-treatment is required; cellulose dissolution is much faster. Additionally, recovery of the IL is feasible, either by removing the volatiles under reduced pressure, or by a salting-out scheme (Fidale et al. 2009). Our results call for more work to test the effects of alternative DAS and other IL-anions on the dissolution and reactivity of cellulose.

Acknowledgments We thank TWAS (The Academy of Sciences for the Developing World) and CNPq (National Council for Scientific and Technological Research) for a pre-doctoral fellowship to H. Nawaz, an undergraduate fellowship to T. A. Bioni, and a productivity fellowship to O. A. El Seoud, and FAPESP (São Paulo research Foundation) for financial support.

References

Ananikov VP (2011) Characterization of molecular systems and monitoring of chemical reactions in ionic liquids by nuclear magnetic resonance spectroscopy. Chem Rev 111:418–454

Anslyn EV, Dougherty DA (2006) Modern physical organic chemistry. University Science Books, Sausalito, p 382

Armagero WLF, Chai CLL (2003) Purification of laboratory chemicals, 5th edn. Elsevier, New York

Arvela PM, Anugwom I, Virtanen P, Sjöholma R, Mikkola JP (2010) Dissolution of lignocellulosic materials and its constituents using ionic liquids—a review. Ind Crops Prod 32:175–201

ASTM D1795-94 (2001) Standard test methods for intrinsic viscosity of cellulose

ASTM D871-96 (2002) Standard test methods of testing cellulose acetate (solution method; procedure A)

Bayly CI, Cieplak P, Cornell WD, Kollman PA (1993) A well-behaved electrostatic potential based method using charge restraints for deriving atomic charges: the RESP model. J Phys Chem 97:10269–10280

Berry RS, Rice SA, Ross J (2000) Journal of Physics Chemistry. Oxford University Press, Oxford, p 524

Bester-Rogac M, Stopp A, Johannes HJ, Hefter G, Buchner R (2011) Association of ionic liquids in solution: a combined dielectric and conductivity study of [bmim][Cl] in water and in acetonitrile. Phys Chem Chem Phys 13:17588–17598

Bruice TC (2006) Computational approaches: reaction trajectories, structures, and atomic motions. Enzyme reactions and proficiency. Chem Rev 106:3119–3139

Buschle-diller G, Zeronian SH (1992) Enhancing the reactivity and strength of cotton fibres. J Appl Polym Sci 45:967–979

Caleman C, van Maaren PJ, Hong M, Hub JS, Costa LT, Van der Spoel D (2012) Force field benchmark of organic liquids: density, enthalpy of vaporization, heat capacities, surface tension, isothermal compressibility, volumetric expansion coefficient, and dielectric constant. J Chem Theory Comput 8:61–74

Catalán J (2009) Toward a generalized treatment of the solvent effect based on four empirical scales: dipolarity (SdP, a new scale), polarizability (SP), acidity (SA), and basicity (SB) of the medium. J Phys Chem B 113:5951–5960

Ciocirlan O, Croitoru O, Iulian O (2011) Densities for binary mixtures of 1-butyl-3-methylimidazolium tetrafluoroborate ionic liquid with molecular solvents. J Chem Eng Data 56:1526–1534

Crosthwaite JM, Aki SNVK, Maginn EJ, Brennecke JF (2005) Liquid phase behavior of imidazolium-based ionic liquids with alcohols: effects of hydrogen bonding and non-polar interactions. Fluid Phase Equilib 228–229:303–309

Dong K, Zhang SJ, Wang DX, Yao XQ (2006) Hydrogen bonds in imidazolium ionic liquids. J Phys Chem A 110:9775–9782

El Seoud OA (2007) Solvation in pure and mixed solvents: some recent developments. Pure Appl Chem 79:1135–1151

El Seoud OA (2009) Understanding solvation. Pure Appl Chem 81:697–707

El Seoud OA, Koschella A, Fidale LC, Dorn S, Heinze T (2007) Applications of ionic liquids in carbohydrate chemistry: a window of opportunities. Biomacromolecules 8:2629–2647

El Seoud OA, Nawaz H, Arêas EPG (2013) Chemistry and applications of polysaccharide solutions in strong electrolytes/dipolar aprotic solvents: an overview. Molecules 18:1270–1313

Fidale LC, Ruiz N, Heinze T, El Seoud OA (2008) Cellulose swelling by aprotic and protic solvents: what are the similarities and differences? Macromol Chem Phys 209:1240–1254

Fidale LC, Possidonio S, El Seoud OA (2009) Application of 1-allyl-3-(1-butyl) imidazolium chloride in the synthesis of cellulose esters: properties of the ionic liquid, and comparison with other solvents. Macromol Biosci 9:813–821

Gericke M, Liebert T, El Seoud OA, Heinze T (2011) Tailored media for homogeneous cellulose chemistry: ionic liquid/CO-solvent mixtures. Macromol Mater Eng 296:483–493

Gericke M, Fardim P, Heinze T (2012) Ionic liquids-promising but challenging solvents for homogeneous derivatization of cellulose. Molecules 17:7458–7502

Gomes TCF, Skaf MS (2012) Cellulose-builder: a toolkit for building crystalline structures of cellulose. J Comput Chem 33:1338–1346

Hanbin L, Kenneth L, Holmes BM, Simmons BA, Singh S (2010) Understanding the interactions of cellulose with ionic liquids: a molecular dynamics study. J Phys Chem B 114:4293–4301

Hauru LKJ, Hummel M, King AWT, Kilpeläinen I, Sixta H (2012) Role of solvent parameters in the regeneration of cellulose from ionic liquid solutions. Biomacromolecules 13:2896–2905

Hesse-Ertelt S, Heinze T, Kosan B, Schwikal K, Meister F (2010) Solvent effects on the NMR chemical shifts of imidazolium-based ionic liquids and cellulose therein. Macromol Symp 294-II:75–89

Humphrey W, Dalke A, Schulten K (1996) VMD—Visual molecular dynamics. J Mol Graphics 14:33–38

Jain RK, Agnish SL, Lal K, Bhatnagar HL (1985) Reactivity of hydroxyl groups in cellulose towards chloro(*p*-tolyl) methane. Makromol Chem 186:2501–2512

Jiang JC, Lin KH, Li SC, Pao-Ming SPM, Hung KC, Lin SH, Chang HC (2011) Association structures of ionic liquid/

DMSO mixtures studied by high-pressure infrared spectroscopy. J Chem Phys 134:044506

Jorgensen WL, Maxwell DS, Tirado-Rives J (1996) Development and testing of the OPLS all-atom force field on conformational energetics and properties of organic liquids. J Am Chem Soc 118:11225–11236

Kwatra HS, Caruthers JM, Tao BY (1992) Synthesis of long chain fatty acids esterified onto cellulose via the vacuum-acid chloride process. Ind Eng Chem Res 31:2647–2651

Le KA, Sescousse R, Budtova T (2012) Influence of water on cellulose-EMIMAc solution properties: a viscometric study. Cellulose 19:45–54

Lide DR (2004) CRC Handbook of chemistry and physics, 85th edn. CRC Press, Boca Raton

Makowska A, Dyoniziak E, Siporska A, Szydlowski J (2010) Miscibility of ionic liquids with polyhydric alcohols. J Phys Chem B 114:2504–2508

Malm CJ, Tanghe LO, Laird BC, Smith GD (1953) Relative rates of acetylation of the hydroxyl groups in cellulose acetate. J Am Chem Soc 75:80–84

Martínez L, Andrade R, Birgin EG, Martínez JM (2009) Packmol: a package for building initial configurations for molecular dynamics simulations. J Comput Chem 30:2157–2164

Nawaz H, Casarano R, El Seoud OA (2012) First report on the kinetics of the uncatalyzed esterification of cellulose under homogeneous reaction conditions: a rationale for the effect of carboxylic acid anhydride chain-length on the degree of biopolymer substitution. Cellulose 19:199–207

Nawaz H, Pires PAR, El Seoud OA (2013) Kinetics and mechanism of imidazole-catalyzed acylation of cellulose in LiCl/*N*, *N*-dimethylacetamide. Carbohydr Polym 92: 997–1005

Neese F, Becker U, Ganiouchine D, Kobmann S, Petrenko T, Riplinger C (2011) Orca - an ab initio, DFT and semiempirical SCF-MO package (Version 2.9). Germany: University of Bonn

Perepelkin KE (2007) Lyocell fibers based on direct dissolution of cellulose in *N*-methylmorpholine *N*-oxide: development and prospects. Fiber Chem 39:163–172

Pinkert A, Marsh KN, Pang S, Staiger MP (2009) Ionic liquids and their interaction with cellulose. Chem Rev 109:6712–6728

Possidonio S, Fidale LC, El Seoud OA (2010) Microwave-assisted derivatization of cellulose in an ionic liquid: an efficient, expedient synthesis of simple and mixed carboxylic esters. J Polym Sci Part A Polym Chem 48:134–143

Press WH, Teukolsky SA, Vetterling WT, Flannergy BP (2007) Numerical recipes: the art of scientific computing, 3rd edn. Cambridge University Press, Cambridge

Punyiczki M, Rosenberg A (1992) The effect of viscosity on the accessibility of the single tryptophan in human serum albumin. Biophys Chem 42:93–100

Sashina ES, Novoselov NP, Kuzmina OG, Troshenkova SV (2008) Ionic liquids as new solvents of natural polymers. Fibre Chem 40:270–277

Sato BM, Oliveira CG, Clarissa TM, El Seoud OA (2010) Thermo-solvatochromism in binary mixtures of water and ionic liquids: on the relative importance of solvophobic interactions. Phys Chem Chem Phys 12:1764–1771

Sato BM, Martins CT, El Seoud OA (2012) Solvation in aqueous binary mixtures: consequences of the hydrophobic character of the ionic liquids and the solvatochromic probes. New J Chem 2353–2360

Silva AWS, Vranken WF (2012) ACPYPE—AnteChamber PYthon Parser interfacE. BMC Res Notes 5:367

Sitnitsky AE (2008) Solvent viscosity dependence for enzymatic reactions. Physica A 387:5483–5497

Somogyi B, Norman JA, Zempel L, Rosenberg A (1988) Viscosity and transient solvent accessibility Trp-63 in the native confirmation of lysozyme. Biophys Chem 32:1–13

Tada EB, Novaki LP, El Seoud OA (2000) Solvatochromism in pure and binary solvent mixtures: effects of the molecular structure of the zwitterionic probe. J Phys Org Chem 13:679–687

Tosh B, Saikia CN, DASs NN (2000) Homogeneous esterification of cellulose in the lithium chloride-*N*, *N*-dimethylacetamide solvent system: effect of temperature and catalyst. Carbohydr Res 327:345–352

Van der Spoel D, Lindahl E, Hess B, Groenhof G, Mark AE, Berendsen HJ (2005) GROMACS: fast, flexible and free. J Comput Chem 26:1701–1718

Vanquelef E, Simon S, Marquant G, Garcia E, Klimerak G, Delepine JC (2011) R.E.D. Server: a web service for deriving RESP and ESP charges and building force field libraries for new molecules and molecular fragments. Nucleic Acids Res (Web server issue) 39:W511–W517

Wang J, Wang W, Kollman PA, Case DA (2004) Development and testing of a general amber force field. J Comput Chem 25:1157–1174

Wang J, Wang W, Kollman PA, Case DA (2006) Automatic atom type and bond type perception in molecular mechanical calculations. J Mol Graph Model 25:247–260